CAPE is predictable from large-scale environmental parameters

Funing Li[1], **Daniel R. Chavas**[1]

[1]Purdue University, Department of Earth, Atmospheric, and Planetary Sciences, West Lafayette, IN

Key Points:

- CAPE can be predicted from environmental sounding parameters without lifting a hypothetical air parcel
- A step-by-step derivation demonstrates how CAPE scales with a recently-proposed CAPE-like quantity
- A simple predictive linear equation is presented based on 20 years of reanalysis data over the U.S.

Corresponding author: Funing Li, li3226@purdue.edu

Abstract

A recent study by Agard and Emanuel (2017) proposed a simple equation for a quantity that scales with convective available potential energy (CAPE) that can be directly calculated from a limited number of environmental sounding parameters without lifting a hypothetical air parcel. This scaling CAPE was applied in a specific idealized framework, but the extent to which it can predict true CAPE in the real world has not been tested. This work uses reanalysis data over the U.S to demonstrate that this scaling CAPE does indeed scale very closely with CAPE, following a linear relationship with a scaling factor of 0.44. We then explain why they scale together via a step-by-step derivation of the theoretical assumptions linking scaling CAPE and real CAPE and their manifestation in the historical data. Overall, this work demonstrates that CAPE can be predicted from large-scale environmental parameters alone, which may be useful for a wide range of applications in weather and climate.

Plain Language Summary

Convective available potential energy (CAPE) is a key parameter commonly used to measure the potential for thunderstorms. Its calculation requires lifting a hypothetical air parcel through a column of atmosphere. This work combines theory and reanalysis data to demonstrate that CAPE can be predicted using environmental data alone. This can make it easier to quickly estimate CAPE in data and to understand the processes that create CAPE in our atmosphere.

1 Introduction

Convective available potential energy (CAPE), a measure of conditional instability of the environment, is a key thermodynamic parameter in atmospheric research. It is proportional to the theoretical maximum vertical wind speed within the atmospheric column, and hence serves as an indicator of the potential for triggering deep convection (Holton, 1973). In practice, regular CAPE is estimated by the vertically-integrated buoyancy of a boundary-layer parcel ascending from the level of free convection (LFC) to the equilibrium level (EL) (Doswell III & Rasmussen, 1994), given by

$$CAPE = \int_{z_{LFC}}^{z_{EL}} g \frac{T_{vp} - T_{ve}}{T_{ve}} dz \tag{1}$$

where g is the acceleration due to gravity, z is height above ground level, T_{vp} is the virtual temperature of the rising air parcel and T_{ve} is that of the surrounding environment. Thus, calculating CAPE requires lifting a hypothetical parcel through a column of atmosphere defined by known vertical profiles of air temperature and moisture.

Recently, Agard and Emanuel (2017, hereafter AE17) proposed a simple equation for a quantity that scales with CAPE, here denoted CAPE_{AE17}, based on an idealized two-layer model for the atmospheric column. The AE17 model includes a dry adiabatic free troposphere overlying a cooler, moist, well-mixed boundary layer. Their proposed quantity scales with the difference between surface moist static energy (M_{ve}^{sfc}) and free tropospheric dry static energy ($\overline{D_{ve}^{FT}}$) multiplied by difference in the natural logarithm of virtual temperatures between boundary-layer top (T_{ve}^{BLT}) and tropopause (T_{ve}^{trop}):

$$CAPE_{AE17} = (M_{ve}^{sfc} - \overline{D_{ve}^{FT}}) ln \frac{T_{ve}^{BLT}}{T_{ve}^{trop}} \tag{2}$$

The D_{ve} and M_{ve} are given by $D_{ve} = c_p T_{ve} + gz$ and $M_{ve} = c_p T_{ve} + gz + L_v r$, respectively, where c_p and L_v are the specific heat of air and the latent heat of vaporization of water, and r is the water vapor mixing ratio. Note that Eq.2 is slightly different from the original formulation in AE17, as we use virtual temperatures rather than temperatures for D_{ve} and M_{ve} to be consistent with definitions of CAPE in Eq.1 (detailed in

Section 3). The CAPE_{AE17} formula suggests that CAPE may to first order be determined by a limited number of environmental parameters within the boundary-layer and free troposphere. One significant benefit of this outcome is that this quantity may be calculated strictly from environmental sounding data without the need to lift a hypothetical air parcel.

Using this idealized framework, AE17 found that peak continental transient CAPE is expected to increase with global warming. Recent work used the AE17 framework to develop a simple physical model for a steady sounding for numerical simulations of severe convective storms (Chavas & Dawson, 2020). However, it remains unclear to what extent CAPE_{AE17} directly predicts true CAPE in real soundings. Moreover, AE17 did not present a formal derivation of the relationship between CAPE_{AE17} and CAPE.

To fill this gap, this work seeks to answer the following question: How closely does CAPE_{AE17} scale with CAPE in real soundings, and why? To answer this question, we first directly compare CAPE_{AE17} with CAPE over the U.S using reanalysis data and show that CAPE_{AE17} does indeed scale closely with regular CAPE (Section 2). We then provide a step-by-step theoretical derivation and application to sounding data to explain why they scale together (Section 3). We end with a summary and discussion (Section 4).

2 CAPE vs. CAPE_{AE17}

We begin with an explicit comparison of CAPE and CAPE_{AE17} in terms of 1) climatological extremes over the U.S, and 2) diurnal evolution during a significant tornado outbreak over the southern U.S.

2.1 Data

We use the 3-hourly surface and model-level (72 vertical levels) Modern-Era Retrospective analysis for Research and Applications version 2 (MERRA-2) reanalysis data for the period 2000–2019 in this work (Gelaro et al., 2017) (data accessed in March 2020 from `https://disc.gsfc.nasa.gov/datasets/M2I1NXASM_5.12.4/summary` for the surface data and from `https://disc.gsfc.nasa.gov/datasets/M2I3NVASM_5.12.4/summary` for the model-level data). The horizontal grid spacing of MERRA-2 is $0.5^\circ \times 0.65^\circ$ in latitude and longitude. MERRA-2 also provides direct estimations of atmospheric properties at boundary-layer top and tropopause, which is especially useful for the calculation of CAPE_{AE17}. Our domain of analysis focuses on the contiguous U.S, as it is a major hot spot for severe thunderstorm environments in the world (Brooks et al., 2003).

We generate a 20-year dataset of CAPE using Eq.1 and CAPE_{AE17} using Eq.2 from the MERRA-2 reanalysis data over the U.S. Though CAPE estimation is sensitive to the origin of air parcel, we select the near-surface parcel defined by 2-m temperature and moisture for simplicity, similar to past work (Riemann-Campe et al., 2009; Seeley & Romps, 2015; Li et al., 2020).

2.2 Results

We first compare the representation of climatological spatial distribution of extreme values of CAPE_{AE17} against CAPE, as strong thunderstorms are typically associated with large values of CAPE. We define extreme values by the 99th percentile of the full-period (2000–2019) time series of a given quantity at each grid point, in line with past work (Singh et al., 2017; Tippett et al., 2016; Li et al., 2020; Taszarek et al., 2020). Results show that extreme CAPE_{AE17} scales very closely with extreme CAPE (Figure 1a; $r = 0.98$), with linear regression given by

$$CAPE \approx 0.44\ (CAPE_{AE17} - 522) \tag{3}$$

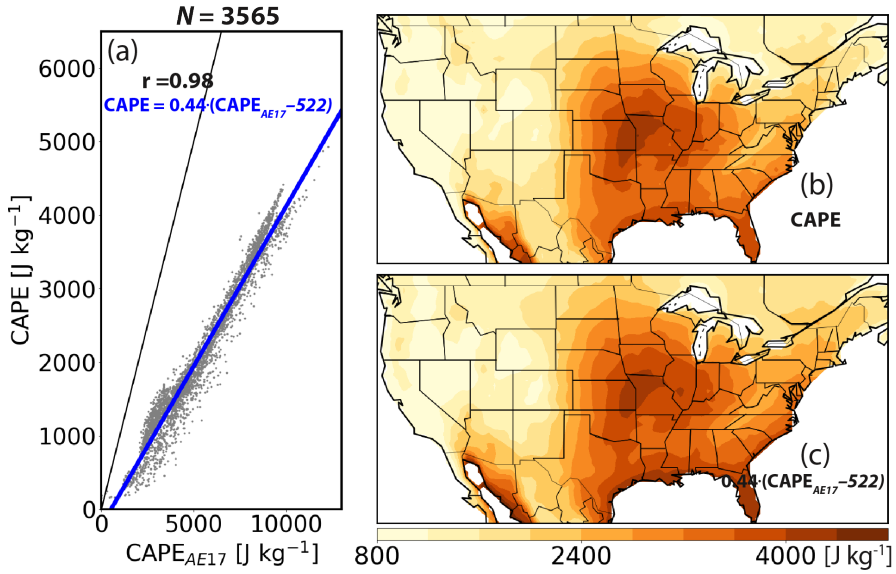

Figure 1. (a) Extreme values of CAPE (Eq.1) vs. CAPE$_{AE17}$ (Eq. 2) over the contiguous U.S. Extreme values are defined as the 99th percentile of their respective full-period (2000–2019) time series from the MERRA-2 reanalysis data at each grid point (gray dots). Sample size is N=3565. Blue line denotes the linear least squares fit with linear correlation coefficient (r). Black line denotes one-to-one fit. (b) Spatial distribution of extreme CAPE. (c) Predicted spatial distribution of extreme CAPE using the linear regression equation shown in (a).

We then apply Eq.3 to predicted extreme CAPE from extreme CAPE$_{AE17}$ (Figure 1c), which produces a spatial pattern that is quantitatively very similar to the observed extreme CAPE (Figure 1b).

To further demonstrate how closely the two quantities scale, we present a case study comparison of their diurnal evolution during April 25, 2011, which is the first day of a three-day significant tornado outbreak event in the southeastern U.S (Knupp et al., 2014). The diurnal variation of CAPE indicates an initial generation of CAPE over southeastern Texas in the early morning (0900–1200 UTC; Figure 2a,b), followed by a strong enhancement at around 1500 UTC over eastern Texas (Figure 2c) and an eastward propagation of high CAPE in the afternoon (Figure 2d–f). The high CAPE values in the afternoon–evening over the southeastern U.S are associated with a swath of over 50 tornado reports extending from eastern Texas into the mid-Mississippi Valley (reference to the SPC Storm Reports: `https://www.spc.noaa.gov/exper/archive/event.php?date=20110425`). Compared to CAPE, CAPE$_{AE17}$ successfully reproduces the detailed spatial patterns and diurnal variations during the day (Figure 2g–l), with pattern correlation $r \geq 0.90$ at each UTC time, though Eq. 3 slightly overestimates CAPE in the morning (Figure 2g,h vs. a,b) and slightly underestimates CAPE in the afternoon (Figure 2j,k vs. d,e).

Overall, our comparisons for both climatological extremes and the diurnal variation associated with a tornado outbreak case demonstrate a tight relationship between CAPE$_{AE17}$ and CAPE distributions. This indicates that CAPE can be approximately predicted from CAPE$_{AE17}$ via a simple linear equation.

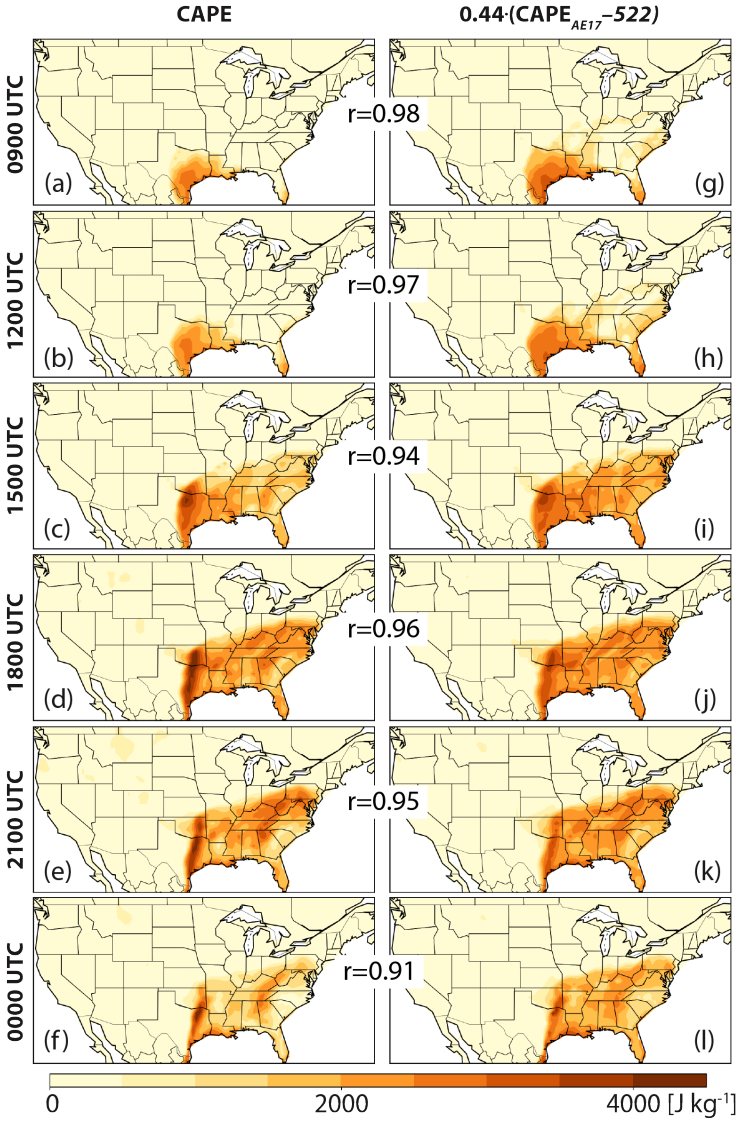

Figure 2. Spatial distributions of (a–f) CAPE vs. (g–l) predicted CAPE, using the equation in Fig 1(a), at (top–bottom) 0900, 1200, 1500, 1800, 2100, and 0000 UTC on April 25, 2011 from the MERRA-2 reanalysis data. The r denotes pattern correlation coefficient between CAPE and CAPE$_{AE17}$ conditioned on gridpoints with CAPE $\geq$ 100 J kg^{-1}.

3 Theoretical foundation

We next provide a theoretical derivation and explanation of the intermediate steps and assumptions that link CAPE to CAPE$_{AE17}$. We demonstrate each step both for a single example radiosonde sounding (Figure 3) and statistically for all U.S gridpoints in the full-period (2000–2019) MERRA-2 reanalysis database (Figure 4). Here the example sounding was observed at 0000 UTC 07 June 2011 at the SGF (Springfield, MO) station; we obtain it from the sounding database of the University of Wyoming (`http://weather.uwyo.edu/upperair/sounding.html`).

3.1 A dry static energy view of CAPE

As CAPE_{AE17} is a function of an environmental static energy deficit between the boundary layer and free troposphere, we first derive an alternative formula for estimating CAPE based on the parcel and environmental profiles of dry static energy rather than temperature.

We begin from the environmental dry static energy relation (D_{ve}), $D_{ve} = c_p T_{ve} + gz$. The environmental moist static energy (M_{ve}) is given by $M_{ve} = c_p T_{ve} + gz + L_v r$. Heat capacities and latent heats are assumed to be constant. Counterparts for the parcel are given by D_{vp} and M_{vp}. Note that these static energies include the virtual temperature effect to be consistent with definitions of CAPE in Eq.1 as shown below. This virtual effect may add a small positive perturbation to regular static energies of approximately 0.9% and 0.8% of near-surface dry and moist static energy, respectively, given a surface temperature of 300 K and mixing ratio of 15 g kg^{-1}, that will decrease with height. We may rewrite the D_{ve} equation for differential changes in height z as $dz = -\frac{c_p}{g} dT_{ve} + \frac{1}{g} dD_{ve}$ and substitute into Eq.1. Doing so yields an alternative formulation of CAPE with limited approximations based on dry static energy profiles of the rising air parcel and the environment (derivation in Appendix A):

$$CAPE \approx \frac{\Gamma_d}{\Gamma}\mathcal{D} = -\frac{\Gamma_d}{\Gamma}\int_{T_{ve}^{LFC}}^{T_{ve}^{EL}} (D_{vp} - D_{ve}) dln T_{ve} \tag{4}$$

where $\Gamma_d = g/c_p$ is the dry adiabatic lapse rate, Γ is the virtual temperature lapse rate of the environment from LFC to EL, and T_{ve}^{LFC} and T_{ve}^{EL} are environmental virtual temperatures at LFC and EL, respectively.

How well does $\frac{\Gamma_d}{\Gamma}\mathcal{D}$ (Eq.4) compare to CAPE (Eq.1)? First, we compare $\frac{\Gamma_d}{\Gamma}\mathcal{D}$ against CAPE for our example sounding (Figure 3 inset). The two calculations yield similar values of CAPE (3775 vs. 3945 J kg^{-1}). Second, we compare the two quantities for all grid-points over the U.S in our MERRA-2 reanalysis dataset. The two quantities are indeed nearly identical (Figure 4a; $r > 0.99$) with linear regression given by CAPE$= 0.98(\frac{\Gamma_d}{\Gamma}\mathcal{D} + 18)$. The $\frac{\Gamma_d}{\Gamma}\mathcal{D}$ formulation performs equally well in reproducing the detailed spatial distribution of extreme CAPE over the U.S (Figure S1b vs. S1a).

3.2 Scaling of CAPE with CAPE_{AE17}

To obtain the CAPE_{AE17} formula from Eq.4, we must assume that $D_{vp} = M_{ve}^{sfc}$, which yields

$$\frac{\Gamma_d}{\Gamma}\mathcal{D}_{AE17} = \frac{\Gamma_d}{\Gamma}(M_{ve}^{sfc} - \overline{D_{ve}}) ln \frac{T_{ve}^{LFC}}{T_{ve}^{EL}} \tag{5}$$

where $\overline{D_{ve}} = \frac{\int_{T_{ve}^{LFC}}^{T_{ve}^{EL}} (D_{ve}) dln T_{ve}}{\int_{T_{ve}^{LFC}}^{T_{ve}^{EL}} dln T_{ve}}$ is the log-temperature-weighted average dry static energy of environment between LFC and EL. Physically, this assumption implies that the lifted air parcel immediately releases all latent heat at LFC. Hence, the parcel will experience a sudden jump in dry static energy D_{vp} (to be equal to M_{vp}) at the LFC, and above the LFC this quantity is conserved. Additionally, we must assume that the moist static energy of the surface parcel is assumed to be conserved up to the LFC. Note that static energy is not perfectly conserved during adiabatic ascent because buoyancy acts as an enthalpy sink (Romps, 2015). Taken together, the assumption results in $D_{vp} = M_{vp} = M_{ve}^{sfc}$.

We use our example sounding (Figure 3) to help understand this assumption conceptually. As noted above, the above assumption implies that all latent heat within an air parcel is immediately converted to sensible heat at the LFC. Thus, the parcel is im-

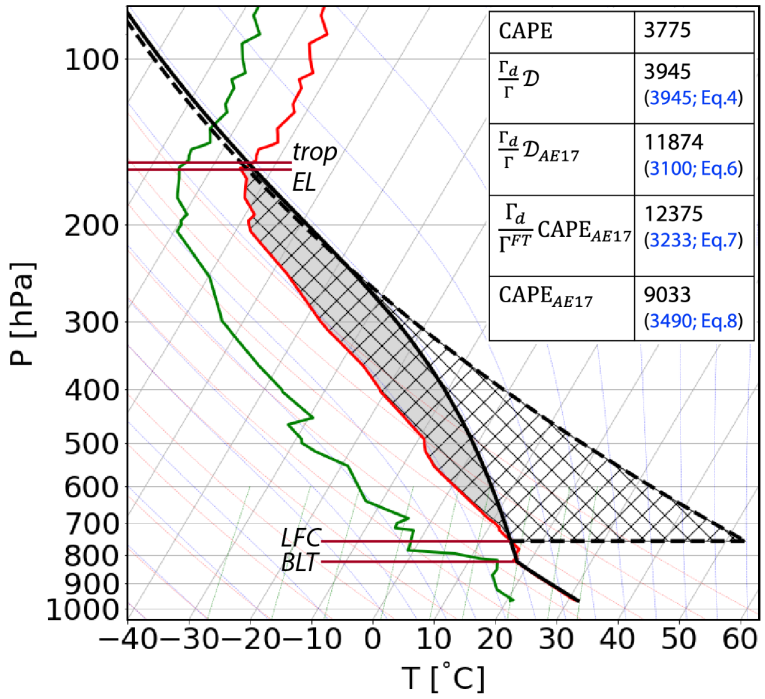

Figure 3. The SGF (Springfield, MO) radiosonde observed virtual temperature (in red line) and dew-point temperature (in green line) profiles at 0000 UTC 07 June 2011 in a Skew-T diagram. Solid black line represents the virtual temperature profile of a surface air parcel ascending adiabatically. Dashed black line represents the modified virtual temperature profile of the parcel ascending assuming that it releases all latent heat immediately at LFC. The *EL*, *LFC*, *trop*, and *BLT* are denoted by brown lines. Inset table lists: CAPE (Eq.1; grey shading); $\frac{\Gamma_d}{\Gamma}\mathcal{D}$ (Eq.4); $\frac{\Gamma_d}{\Gamma}\mathcal{D}_{AE17}$ (Eq.5; hatched); $\frac{\Gamma_d}{\Gamma^{FT}}$CAPE$_{AE17}$ is the same as $\frac{\Gamma_d}{\Gamma}\mathcal{D}_{AE17}$ but using virtual temperatures at *BLT* and *trop*, with CAPE$_{AE17}$ calculated from Eq.2. The inset table lists direct calculation of each quantity (black text) and prediction of true CAPE (blue text) using the relevant linear regression equation. The Python MetPy (May et al., 2008–2020) package is used to generate the parcel temperature profiles.

mediately warmed dramatically at the LFC and then subsequently rises dry adiabatically from the LFC to the EL. In this way, then, $\frac{\Gamma_d}{\Gamma}\mathcal{D}_{AE17}$ is considered a "scaling" CAPE because it represents a theoretical upper bound on how quickly a parcel can be warmed along its path (and hence on its integrated buoyancy). In the real atmosphere, latent heat is released gradually along the parcel path in accordance with the Clausius-Clapeyron relation that defines the moist adiabatic lapse rate. In a Skew-T diagram, this difference shows up as an expanded, angular region of positive buoyancy maximized above the LFC in $\frac{\Gamma_d}{\Gamma}\mathcal{D}_{AE17}$. Thus, $\frac{\Gamma_d}{\Gamma}\mathcal{D}_{AE17}$ is substantially larger than CAPE ($\frac{\Gamma_d}{\Gamma}\mathcal{D}_{AE17}$ =11874 J kg^{-1} vs. CAPE = 3775 J kg^{-1} in Figure 3 inset). Though different in magnitude, $\frac{\Gamma_d}{\Gamma}\mathcal{D}_{AE17}$ is still highly correlated with CAPE (r=0.92) in the full reanalysis dataset over the U.S (Figure 4b), with linear regression given by

$$CAPE \approx 0.32(\frac{\Gamma_d}{\Gamma}\mathcal{D}_{AE17} - 2188) \tag{6}$$

For the example sounding, Eq.6 predicts a CAPE value (3100 J kg^{-1}) that is reasonably close to the true CAPE (3775 J kg^{-1}) (Figure 3 inset). Eq.6 also performs very well in reproducing the spatial distribution of extreme CAPE over the U.S (Figure S1c vs. S1a).

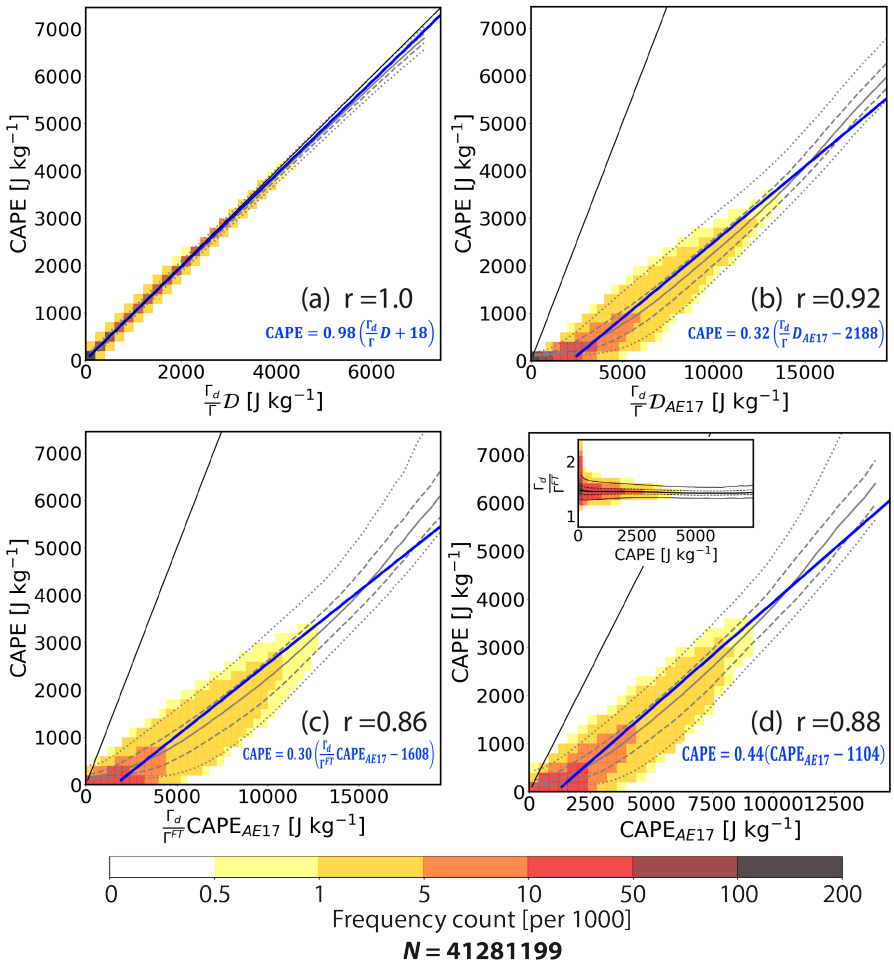

Figure 4. Joint frequency fraction multiplied by 1000 (filled color) of (a) CAPE vs. $\frac{\Gamma_d}{\Gamma}\mathcal{D}$, (b) CAPE vs. $\frac{\Gamma_d}{\Gamma}\mathcal{D}_{AE17}$, (c) CAPE vs. $\frac{\Gamma_d}{\Gamma^{FT}}\text{CAPE}_{AE17}$, and (d) CAPE vs. CAPE_{AE17} (inset: $\frac{\Gamma_d}{\Gamma^{FT}}$ vs. CAPE) for cases with CAPE $\geq$ 100 J kg^{-1} over all U.S gridpoints during 2000–2019 from the MERRA-2 reanalysis dataset (sample size N=41281199). Black line denotes one-to-one line. Gray lines denote median (solid), interquartile range (dashed), and 5–95% range (dotted) of CAPE. Blue line denotes the linear regression with the correlation coefficient of r.

Physically, the factor 0.32 is a manifestation of the rate at which saturation vapor pressure decreases with temperature, as defined by the Clausius-Clapeyron relation, that is fundamental to our real atmosphere.

Finally, to produce a prediction with the original AE17 formulation (CAPE_{AE17}), we must additionally assume that the temperatures of the EL and LFC may be replaced with that of the tropopause (*trop*) and boundary-layer top (BLT), respectively. This replaces $\frac{\Gamma_d}{\Gamma}\mathcal{D}_{AE17}$ of Eq.5 with $\frac{\Gamma_d}{\Gamma^{FT}}\text{CAPE}_{AE17}$, where Γ^{FT} is defined by the lapse rate of virtual temperature of the free troposphere between the BLT and *trop*. These approximations are more quantitatively reasonable for higher-CAPE cases supportive of deep convection, as in the example sounding (Figure 3). This final approximation ($\frac{\Gamma_d}{\Gamma^{FT}}\text{CAPE}_{AE17}$) is estimated solely by environmental parameters without lifting a hypothetical air parcel. We use the reanalysis dataset to examine its relationship to CAPE (Figure 4c), which

indicates a close correlation (r=0.86) with a linear regression given by:

$$CAPE \approx 0.30(\frac{\Gamma_d}{\Gamma^{FT}} CAPE_{AE17} - 1608) \tag{7}$$

Hence the scaling factor is similar to that for $\frac{\Gamma_d}{\Gamma}\mathcal{D}_{AE17}$ above. For our example sounding, Eq.7 predicts a CAPE value (3233 J kg^{-1}) again reasonably close to the true CAPE (3775 J kg^{-1}) (Figure 3 insert). Eq.7 also quantitatively reproduces the spatial pattern of extreme CAPE over the U.S (Figure S1d vs. S1a).

Ultimately, then, Eq.7 offers a scaling of CAPE that depends only on a limited number of boundary-layer and free tropospheric variables. It differs from CAPE$_{AE17}$ itself in the inclusion of the coefficient $\frac{\Gamma_d}{\Gamma^{FT}}$. This factor does not appear in the idealized model of AE17 because their model assumes a dry adiabatic free troposphere (i.e., $\Gamma^{FT} = \Gamma_d$), which yields $\frac{\Gamma_d}{\Gamma^{FT}} = 1$.

Given that CAPE was found to be predictable from CAPE$_{AE17}$ alone in Section 2 (Eq.3), this result implies that the free tropospheric lapse rate (Γ^{FT}) of the modern atmosphere does not vary too strongly and thus the factor $\frac{\Gamma_d}{\Gamma^{FT}}$ remains relatively constant. We use our reanalysis dataset to calculate the statistics of $\frac{\Gamma_d}{\Gamma^{FT}}$ as a function of CAPE (Figure 4d inset). The result is indeed a mean ($\pm$ one standard deviation) value of 1.47$\pm$0.06, with variance decreasing as CAPE increases. The resulting mean free tropospheric lapse rate (Γ^{FT}) is roughly 6.7 K km^{-1}, which is close to that of the U.S Standard Atmosphere (COESA, 1976). As a result, we are able to directly scale CAPE with CAPE$_{AE17}$ by assuming that $\frac{\Gamma_d}{\Gamma^{FT}}$ is constant. We note that this behavior may differ in an alternate climate state. As a final test, we compare CAPE$_{AE17}$ with CAPE for cases with CAPE $\geq$ 100 J kg^{-1} for the entire MERRA-2 database over the U.S and find a strong linear correlation between them as well ($r = 0.88$; Figure 4d), with a linear regression of

$$CAPE \approx 0.44(CAPE_{AE17} - 1104). \tag{8}$$

This outcome is quite similar to the linear regression model we get from extreme cases alone in Eq.3. This is also close to the results of simply substituting $\frac{\Gamma_d}{\Gamma^{FT}}$=1.47$\pm$0.06 into Eq.7, which yields a scaling factor of 0.44$\pm$0.02 and an offset of $-$1095$\pm$50. Using Eq.8 also successfully predicts the approximate CAPE for the example sounding (3490 vs. 3775 J kg^{-1}; Figure 3 inset).

4 Conclusions

CAPE is a key thermodynamic parameter commonly calculated to evaluate the potential for deep convection within a given environment. AE17 proposed a simple formula for a quantity (CAPE$_{AE17}$) that scales with CAPE that depends only on a limited number of environmental variables and does not require lifting a hypothetical parcel.

This work used a 20-year reanalysis dataset over the U.S to examine the extent to which this CAPE-like quantity can be used to predict true CAPE for real soundings, analyzing both the spatial distribution of climatological extremes and the diurnal variation associated with a historical tornado outbreak case study. Results show a close scaling relationship between CAPE$_{AE17}$ and CAPE, yielding a simple linear equation for predicting CAPE from environmental data. To understand the physics underlying this relationship, we provided a step-by-step derivation linking the two quantities, which may be summarized as:

$$CAPE \overset{\text{a1}}{\approx} \frac{\Gamma_d}{\Gamma}\mathcal{D} \overset{\text{a2}}{\simeq} \frac{\Gamma_d}{\Gamma}\mathcal{D}_{AE17} \overset{\text{a3}}{\simeq} \frac{\Gamma_d}{\Gamma^{FT}} CAPE_{AE17} \overset{\text{a4}}{\simeq} CAPE_{AE17} \tag{9}$$

where (a1–a4) represent the assumptions: (a1) constant environmental virtual temperature lapse rate from LFC to EL; (a2) the rising parcel immediately releases all latent

heat at LFC; (a3) temperatures at the EL and LFC scale with the tropopause and boundary-layer top, respectively; (a4) free tropospheric lapse rate of the present atmosphere does not vary strongly in space or time in environments with non-negligible CAPE.

The principal end result of this work is a simple linear equation based on the 20-year reanalysis dataset over the U.S (Eq.8) to predict CAPE from CAPE_{AE17}, which may be calculated strictly from environmental data without the need to lift a hypothetical parcel. This has significant practical benefits for the simple estimation of CAPE and for understanding how CAPE is generated within the climate system.

Appendix A Derivation of Eq.4

The equation for differential changes in environmental dry static energy may be written as $dz = -\frac{c_p}{g} dT_{ve} + \frac{1}{g} dD_{ve}$ and substituting into Eq.1 yields

$$CAPE = \int_{z_{LFC}}^{z_{EL}} g \frac{T_{vp} - T_{ve}}{T_{ve}} (-\frac{c_p}{g} dT_{ve} + \frac{1}{g} dD_{ve}) = \mathcal{D} \; + \; \mathcal{T} \tag{A1}$$

This formulation decomposes CAPE into two terms. The first is given by

$$\mathcal{D} = -\int_{z_{LFC}}^{z_{EL}} (\frac{T_{vp} - T_{ve}}{T_{ve}}) d(c_p T_{ve}) = -\int_{z_{LFC}}^{z_{EL}} (D_{vp} - D_{ve}) dln T_{ve} \tag{A2}$$

and represents differences in dry static energy integrated over changes in temperature. The second is given by

$$\mathcal{T} = \int_{z_{LFC}}^{z_{EL}} (\frac{T_{vp} - T_{ve}}{T_{ve}}) dD_{ve} \tag{A3}$$

and represents integrated differences in temperature over changes in dry static energy. To further simplify Eq.A1, we can relate $\mathcal{T}$ and $\mathcal{D}$ by calculating their ratio. Using the definition of buoyancy, $b = \frac{T_{vp} - T_{ve}}{T_{ve}}$, we may write this ratio as

$$\begin{aligned} \frac{\mathcal{T}}{\mathcal{D}} &= \frac{\int_{z_{LFC}}^{z_{EL}} (b) \; dD_{ve}}{-\int_{z_{LFC}}^{z_{EL}} (b) \; d(c_p T_{ve})} \\ &= -(1 + \frac{g}{c_p} \frac{\int_{z_{LFC}}^{z_{EL}} (b) \; dz}{\int_{z_{LFC}}^{z_{EL}} (b) \; dT_{ve}}) \\ &= -(1 + \frac{g}{c_p} \frac{\overline{b_1} \int_{z_{LFC}}^{z_{EL}} dz}{\overline{b_2} \int_{z_{LFC}}^{z_{EL}} dT_{ve}}) \\ &= \frac{\overline{b_1}}{\overline{b_2}} \frac{\Gamma_d}{\Gamma} - 1 \end{aligned} \tag{A4}$$

where $\overline{b_1} = \frac{\int_{z_{LFC}}^{z_{EL}} (b) \; dz}{\int_{z_{LFC}}^{z_{EL}} dz}$ and $\overline{b_2} = \frac{\int_{z_{LFC}}^{z_{EL}} (b) \; dT_{ve}}{\int_{z_{LFC}}^{z_{EL}} dT_{ve}}$ represent the mean value of b between the LFC and EL weighted by height (z) and environmental virtual temperature (T_{ve}), respectively. $\Gamma_d = g/c_p$ is the dry adiabatic lapse rate and $\Gamma = -\frac{\int_{z_{LFC}}^{z_{EL}} dT_{ve}}{\int_{z_{LFC}}^{z_{EL}} dz} = -\frac{T_{ve}^{EL} - T_{ve}^{LFC}}{z_{EL} - z_{LFC}}$ represents the average environmental virtual temperature lapse rate from LFC to EL.

If we take Γ to be constant between the LFC and EL, then $\overline{b_1} = \overline{b_2}$, which yields

$$\frac{\mathcal{T}}{\mathcal{D}} \;\; = \;\; \frac{\Gamma_d}{\Gamma} - 1 \tag{A5}$$

Substituting this result into Eq.A1 yields

$$CAPE \;\; \approx \;\; \frac{\Gamma_d}{\Gamma} \mathcal{D} = -\frac{\Gamma_d}{\Gamma} \int_{z_{LFC}}^{z_{EL}} (D_{vp} - D_{ve}) dln T_{ve} \tag{A6}$$

This equation is shown to closely match the true CAPE in the main manuscript.

Acknowledgments

The authors acknowledge high-performance computing support from Cheyenne (doi:10.5065/D6RX99HX) provided by NCAR's Computational and Information Systems Laboratory, sponsored by the National Science Foundation, for the data analysis performed in this work. The authors gratefully acknowledge the open-source Python community, and particularly the authors and contributors to the Matplotlib (Hunter, 2007), NumPy (Oliphant, 2006), and MetPy (May et al., 2008–2020) packages that were used to generate many of the figures. Li and Chavas were supported by NASA FINESST grant 12000365 and NSF grant 1648681. The surface and model-level MERRA-2 reanalysis data during 2000–2019 were downloaded from `https://disc.gsfc.nasa.gov/datasets/M2I1NXASM_5.12.4/summary` and `https://disc.gsfc.nasa.gov/datasets/M2I3NVASM_5.12.4/summary`, respectively. The example sounding was obtained from the sounding database of the University of Wyoming at `http://weather.uwyo.edu/upperair/sounding.html`.

References

Agard, V., & Emanuel, K. (2017). Clausius–Clapeyron scaling of peak CAPE in continental convective storm environments. *Journal of the Atmospheric Sciences*, *74*(9), 3043–3054. doi: https://doi.org/10.1175/JAS-D-16-0352.1

Brooks, H. E., Lee, J. W., & Craven, J. P. (2003). The spatial distribution of severe thunderstorm and tornado environments from global reanalysis data. *Atmospheric Research*, *67*, 79–94. doi: https://doi.org/10.1016/S0169-8095(03)00045-0

Chavas, D. R., & Dawson, I., Daniel T. (2020). An idealized physical model for the severe convective storm environmental sounding. *Journal of the Atmospheric Sciences*, 1-62. doi: https://doi.org/10.1175/JAS-D-20-0120.1

COESA. (1976). U.S. Standard Atmosphere. *National Oceanic and Atmospheric Administration*, *76*(1562), 227pp.

Doswell III, C. A., & Rasmussen, E. N. (1994). The effect of neglecting the virtual temperature correction on CAPE calculations. *Weather and forecasting*, *9*(4), 625–629. doi: https://doi.org/10.1175/1520-0434(1994)009⟨0625:TEONTV⟩2.0.CO;2

Gelaro, R., McCarty, W., Suárez, M. J., Todling, R., Molod, A., Takacs, L., ... others (2017). The modern-era retrospective analysis for research and applications, version 2 (MERRA-2). *Journal of Climate*, *30*(14), 5419–5454. doi: https://doi.org/10.1175/JCLI-D-16-0758.1

Holton, J. R. (1973). An introduction to dynamic meteorology. *American Journal of Physics*, *41*(5), 752–754.

Hunter, J. D. (2007). Matplotlib: A 2d graphics environment. *Computing in Science & Engineering*, *9*(3), 90–95. doi: 10.1109/MCSE.2007.55

Knupp, K. R., Murphy, T. A., Coleman, T. A., Wade, R. A., Mullins, S. A., Schultz, C. J., ... others (2014). Meteorological overview of the devastating 27 April 2011 tornado outbreak. *Bulletin of the American Meteorological Society*, *95*(7), 1041–1062. doi: https://doi.org/10.1175/BAMS-D-11-00229.1

Li, F., Chavas, D. R., Reed, K. A., & Dawson II, D. T. (2020). Climatology of severe local storm environments and synoptic-scale features over North America in ERA5 reanalysis and CAM6 simulation. *Journal of Climate*. doi: https://doi.org/10.1175/JCLI-D-19-0986.1

May, R. M., Arms, S. C., Marsh, P., Bruning, E., Leeman, J. R., Goebbert, K., ... Bruick, Z. S. (2008–2020). *Metpy: A Python package for meteorological data.* Boulder, Colorado: Unidata. doi: 10.5065/D6WW7G29

Oliphant, T. E. (2006). *A guide to NumPy* (Vol. 1). Trelgol Publishing USA.

Riemann-Campe, K., Fraedrich, K., & Lunkeit, F. (2009). Global climatology of convective available potential energy (CAPE) and convective inhibition (CIN) in ERA-40 reanalysis. *Atmospheric Research*, *93*(1-3), 534–545. doi:

https://doi.org/10.1016/j.atmosres.2008.09.037

Romps, D. M. (2015). MSE Minus CAPE is the True Conserved Variable for an Adiabatically Lifted Parcel. *Journal of the Atmospheric Sciences*, *72*(9), 3639-3646. doi: https://doi.org/10.1175/JAS-D-15-0054.1

Seeley, J. T., & Romps, D. M. (2015). The effect of global warming on severe thunderstorms in the United States. *Journal of Climate*, *28*(6), 2443–2458. doi: https://doi.org/10.1175/JCLI-D-14-00382.1

Singh, M. S., Kuang, Z., Maloney, E. D., Hannah, W. M., & Wolding, B. O. (2017). Increasing potential for intense tropical and subtropical thunderstorms under global warming. *Proceedings of the National Academy of Sciences*, *114*(44), 11657–11662. doi: https://doi.org/10.1073/pnas.1707603114

Taszarek, M., Allen, J. T., Púčik, T., Hoogewind, K. A., & Brooks, H. E. (2020). Severe convective storms across Europe and the United States. Part 2: ERA5 environments associated with lightning, large hail, severe wind and tornadoes. *Journal of Climate*, 1–53. doi: https://doi.org/10.1175/JCLI-D-20-0346.1

Tippett, M. K., Lepore, C., & Cohen, J. E. (2016). More tornadoes in the most extreme US tornado outbreaks. *Science*, *354*(6318), 1419–1423. doi: https://doi.org/10.1126/science.aah7393